

Algorithm Description Ver.2.1 (Revision 2017.3.31)

PI No. 302 Takafumi Hirata (GCOM-C/SGLI Ocean Team)

Theoretical Description of the Euphotic Depth Algorithm

1. Physics of the problem

The euphotic depth $z_{1\%}$ is defined as the depth z at which the photosynthetically available radiation (PAR) at the sea surface falls to 1% of that (i.e. $PAR(z_{1\%}) = 0.01 PAR(z=0^-)$, where 0- indicates “just below the sea surface”). The PAR is defined by $PAR(z) = \int E_0(z, \lambda) d\lambda$ where $400 \leq \lambda \leq 700\text{nm}$, and $E_0(z, \lambda)$ here represents the spectral scalar irradiance. PAR is attenuated with depth by:

$$PAR(z) = PAR(z=0) \exp(-\int K_{PAR}(z) \cdot dz) = PAR(z=0) \exp(-\overline{K_{PAR}} \cdot z). \quad (1)$$

$\overline{K_{PAR}}$ is the depth average of the diffuse attenuation coefficient for PAR:

$$\overline{K_{PAR}} = \int K_{PAR}(z) dz / \int 1 dz = \int K_{PAR}(z) dz / z$$

and $K_{PAR}(z)$, which is a function of depth, is defined by:

$$K_{PAR}(z) = d(\ln PAR(z)) / dz.$$

From Eq. 1, we obtain

$$z_{1\%} = -\ln[PAR(z=z_{1\%})/PAR(z=0)] / \int K_{PAR}(z) dz = -\ln(0.01) / \overline{K_{PAR}} \quad (2)$$

Equation (2) indicates that $z_{1\%}$ is found when $\overline{K_{PAR}}$ is known. Therefore, $\overline{K_{PAR}}$ is a key factor to

estimate $z_{1\%}$. In the following section, a derivation of $\overline{K_{PAR}}$ (hence $z_{1\%}$) using a remote measurement of the radiance is shown. Essentially, the problem is composed of the four practical problems (i) How a conventional approximation of K_{PAR} can be corrected to represent the exact K_{PAR} for a better estimation of $z_{1\%}$, (ii) How the spectrally-integrated quantity of K_{PAR} is derived from a radiance measured remotely at a limited number of discrete wavelengths, (iii) How a depth average of K_{PAR} is derived from K_{PAR} at the surface which a remote sensor would detect, (iv) How K_{PAR} at the

surface can actually be derived from the remotely-sensed radiance. In the following, wavelength- and depth dependencies of the variables such as PAR and K_{PAR} are omitted unless otherwise specified.

2. Euphotic Depth Algorithm

2.1 How the spectrally-integrated property of K_{PAR} is derived from a limited numbers of discrete wavelengths?

The diffuse attenuation coefficient for PAR ($K_{PAR}(\lambda, z)$) is related to that of the spectral scalar irradiance $K_0(\lambda, z)$ via

$$\begin{aligned}
 K_{PAR}(z) &= -\frac{1}{\int_{400}^{700} E_0(\lambda, z) d\lambda} \frac{d\left(\int_{400}^{700} E_0(\lambda, z) d\lambda\right)}{dz} \\
 &= -\frac{1}{300 \overline{E_0(\lambda, z)}} \frac{d\left(300 \overline{E_0(\lambda, z)}\right)}{dz} \\
 &= K_0(\lambda', z)
 \end{aligned} \tag{4}$$

where λ' is a wavelength at which $\overline{E_0(\lambda, z)} = E_0(\lambda', z)$ or $PAR(z) = 300 E_0(\lambda', z)$ is found. It shows that $K_{PAR}(z)$ can be calculated from $K_0(\lambda'z)$ for any z , once if λ' is known.

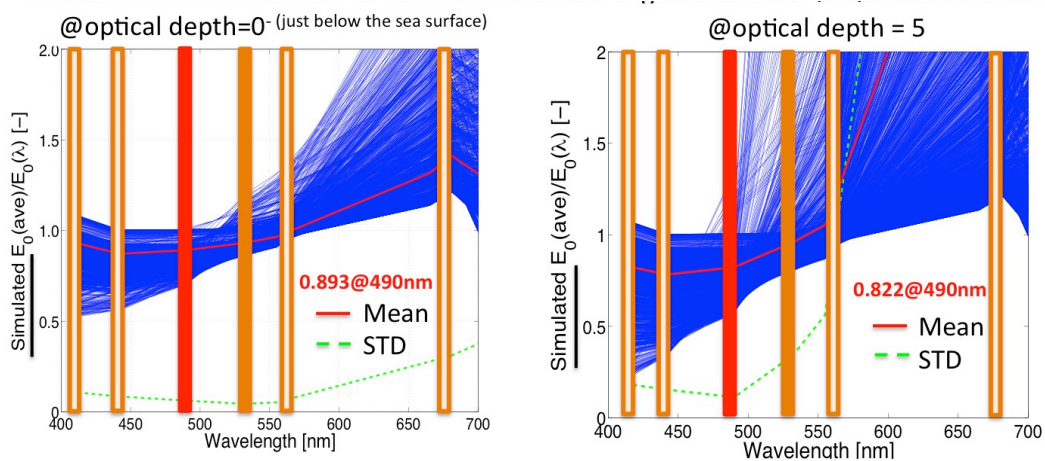


Fig. 1 The ratio of the spectral average of E_0 to $E_0(\lambda)$ for the optical depth of 0 (left) and 5 (right).

Fig. 1 shows the ratio between $\overline{E_0(\lambda,z)}$ and $E_0(\lambda,z)$, derived from the radiative transfer simulation (Appendix A). The wavelength at which this ratio equals unity is found as λ' . At the sea surface (or the optical depth = 0), $\overline{E_0(\lambda,z)}$ is often close to $E_0(\lambda,z)$ numerically at $\lambda=560\text{nm}$, so that λ' is often 560nm, although λ' does vary. The same holds true for the optical depth of 5.0 (which is close to the optical depth of 4.6 and corresponds to z1%). However, uncertainty of the ratio at 560nm represented by the standard deviation (hence, uncertainty of λ') is also large at the optical depth of 5.0. Rather, the uncertainty is small between 412-490nm at both the optical depth of 0.0 and 5.0 (and intermediate depths not shown), although the ratio is no longer unity (i.e. $\overline{E_0(\lambda,z)} \neq E_0(\lambda,z)$). Over the water column considered (i.e. the optical depth 0 to 5.0), we found that the uncertainty is smallest at the wavelength of 490 nm, with $\overline{E_0(\lambda,z)}/E_0(\lambda,z)=0.835 \pm 0.04$ among SGLI Visible and Near Infrared Radiometer wavelengths (i.e. 412, 443, 490, 530, 565, 673, 763, 868nm). Although the ratio is not unity, $\overline{E_0(\lambda,z)}$ can be estimated by using 490nm more successfully than λ' because, even if the ratio is 0.835, Eq. 4 can be re-written by

$$\begin{aligned}
 K_{PAR}(z) &= -\frac{1}{300 \cdot \overline{E_0(\lambda,z)}} \frac{d(300 \cdot \overline{E_0(\lambda,z)})}{dz} \\
 &= -\frac{1}{257.4 \cdot E_0(490,z)} \frac{d(257.4 \cdot E_0(490,z))}{dz} \\
 &= K_0(490,z)
 \end{aligned}
 \tag{4'}$$

to reach the same conclusion as Eq. 4 that K_{PAR} can be found directly from K_0 for any z . At a glance, it then seems in Eq. 4' that a choice of the wavelength doesn't matter, as any value of the ratio between $\overline{E_0(\lambda,z)}$ and $E_0(\lambda,z)$ will be canceled out in Eq. 4' to always reach the same conclusion of $K_{PAR}(z)=K_0(z)$. Given that λ' is more or less variable and cannot be predicted easily (see Fig. 1), it is the stability and uncertainty of the ratio in various environmental conditions, not the ratio value itself, that affects the robustness of the replacement of $\overline{E_0(\lambda,z)}$ with $E_0(\lambda,z)$, hence the validity of the

conclusion from Eq. 4(4'). Since a choice of wavelength affects the stability and uncertainty, the choice must carefully be made, unless one can always know and change in advance the variable wavelength that gives the best estimate of $\overline{E_0(\lambda, z)}$ and can find the wavelengths within a constrain of satellite sensor bands (i.e. a limited numbers of sensor wavelengths). From Eq. 4', it is obvious that $K_{PAR} = K_0(490)$ for $z=0$.

2.1 How a depth average of K_{PAR} is derived from K_{PAR} at the surface?

Fig. 2a shows vertical profiles of $K_0(490, z)$ ($=K_{PAR}(z)$, see Eq. 4'). Depending on the solar zenith angle θ_s , $K_0(490, z)$ varies with depth over 9%, even if the inherent optical properties of water body remain uniform over the water column. Thus, the approximation of $K_0(490, 0) = K_0(490, z)$ (hence, $K_{PAR}(0) = K_{PAR}(z)$) would lead to an inneligious error and must be corrected.

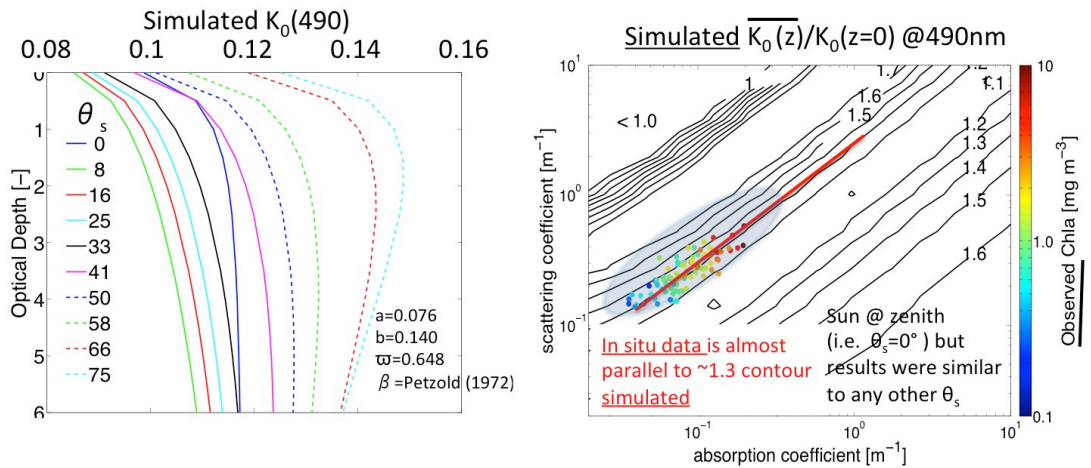


Fig.2 K_0 at 490 nm as a function of the optical depth (left) and the ratio of the depth average of $K_0(490)$ to the surface value of $K_0(490)$.

Fig.2b shows the ratio between $\overline{K_0(490, z)}$ and $K_0(490, z)$ at $\theta_s=0^\circ$, as a function of the optical properties (i.e. the absorption and the scattering coefficients) of bulk water. This result was similar to those at other θ_s , hence not shown. At realistic combinations of the absorption and scattering coefficients obtained from in situ measurements (NOMAD, Werdell et al. 2005), variability in the ratio is rather confined to a narrow range, namely 1.35 ± 0.05 , so that

$$\overline{K_{PAR}(z)} = \overline{K_0(490, z)} = (1.3 \pm 0.05) \cdot K_0(490, 0). \quad (5)$$

The next step is to find $K_0(490, 0)$ from a remote measurement of the radiance. This may involve

two scientific challenges in our strategy; (1) How $K_0(490,0)$ can be related to a routinely evaluated variable such as $K_d(490,0)$ and (2) How $K_d(490,0)$ can be found from the remotely-sensed radiance.

To proceed, we define the ratio between the scalar irradiance E_0 to the downward scalar irradiance E_{od} so that $E_0(\lambda,z) = \varepsilon_1(\lambda,z) E_{od}(\lambda,z)$. We also define the average cosine for the downward radiance $\mu_d(\lambda,z) = E_d(\lambda,z)/E_{od}(\lambda,z)$. For simplicity, the wavelength- and depth dependency of these variables are omitted hereafter unless otherwise specified. As in the case for $K_0(\lambda,z)$ (and $K_{PAR}(\lambda,z)$, etc), the diffuse attenuation coefficient for ε_1 and $\mu_d(\lambda,z)$ can be defined as $K_{\varepsilon_1}(\lambda,z) = -(1/\varepsilon_1(\lambda,z)) (d\varepsilon_1(\lambda,z)/dz)$ and $K_{\mu_d}(\lambda,z) = -(1/\mu_d(\lambda,z)) (d\mu_d(\lambda,z)/dz)$, respectively. As a result, we get

$$\begin{aligned}
K_0(490,0) &= -\frac{1}{\varepsilon_1(z,\lambda) \cdot E_{od}(z,\lambda)} \frac{d(\varepsilon_1(490,0) \cdot E_{od}(490,0))}{dz} \\
&= -\frac{\mu_d(490,0)}{\varepsilon_1(490,0) \cdot E_{od}(490,0)} \frac{d(\varepsilon_1(490,0) \cdot E_d(490,0) / \mu_d(490,0))}{dz} \\
&= K_d(490,0) + K_{\varepsilon_1}(490,0) - K_{\mu_d}(490,0) \\
&= K_d(490,0) + \Delta K(490,0)
\end{aligned}$$

(6)

where $\Delta K(490,0) = K_{\varepsilon_1}(490,0) - K_{\mu_d}(490,0)$. At a glance, $K_0(490,0)$ is linearly related to $K_d(490,0)$ in this expression (although $\Delta K(490,0)$ may or may not be a function of $K_d(490,0)$, which we do not know at this point). In order to find a relationship between $K_0(490,0)$ and $K_d(490,0)$, Fig. 3 is plotted to show their ratio at $z=0$ as a function of the absorption and scattering coefficients of bulk water bodies for different solar angles $\theta_s = 0^\circ$ (Fig. 3b) and 50° (Fig. 3c). For realistic combinations of the absorption and scattering represented by in situ data, the ratio tends to lie on a contour of 0.80 and 0.98, respectively. This suggests that $K_0(490,0)$ co-varies with $K_d(490,0)$ for different water bodies (i.e. for different combination of the absorption and scattering), although $K_0(490,0) \neq K_d(490,0)$ necessarily. Also shown in Fig. 3c is the ratio at 490nm varying with θ_s , which can mathematically be formulated by

$$\begin{aligned}
K_0(490,0) &= K_d(490,0) - [K_d(490,0) \cdot 0.201 \cdot \exp(-0.043\theta_s)] \\
&= K_d(490,0) + \Delta K'(490,0)
\end{aligned}$$

(7)

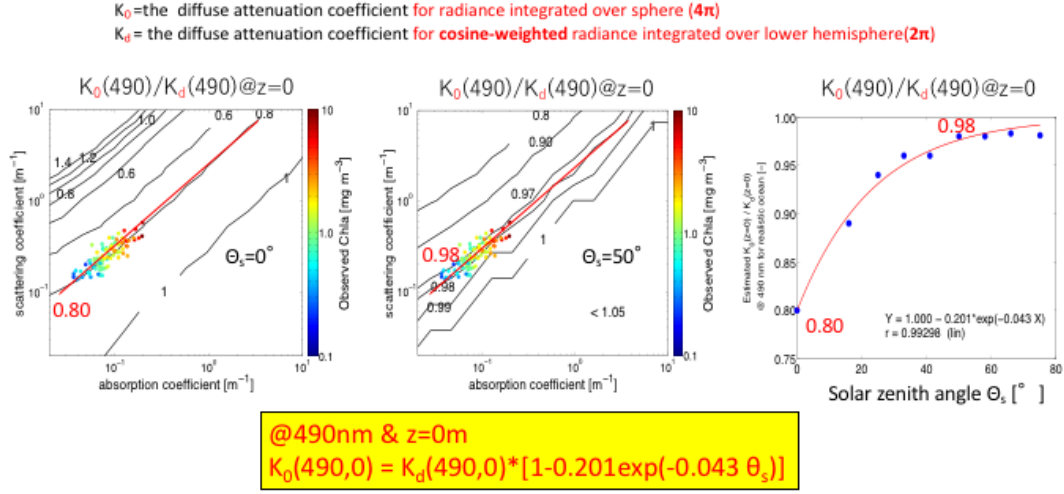


Fig. 3 The ratio of K_0 ($\lambda=490\text{nm}$, $z=0\text{m}$) to $K_d(490,0)$ for $\theta_s=0^\circ$ (left) and $\theta_s=50^\circ$ (center), and the solar dependency of the ratio (right).

Comparison between Eqs. 6 and 7 suggests $\Delta K = \Delta K'$, so that ΔK can be expressed as a function of K_d :

$$\Delta K(490,0) = \Delta K'(490,0) = K_d(490,0) \cdot 0.201 \cdot \exp(-0.043\theta_s). \quad (8)$$

From Eq. 7, $K_0(490,0)$ can be expressed by only $K_d(490)$ for a given θ_s (i.e. for a given observation condition). From the two-flow radiative transfer model (Hirata et al., 2008) for a homogenous water (i.e. inherent optical properties of water body is uniform over the water column), $K_d(490,0)$ may be expressed by

$$\begin{aligned}
 K_d(490,0) &= \frac{c - r_{dd}b_f}{\mu_d} - \frac{r_{ud}b_b R}{\mu_u} \\
 &= \varepsilon_2 \frac{a + b_b}{\mu_d}
 \end{aligned} \quad (9)$$

where the beam attenuation coefficient is denoted by c , the forward- and backscattering coefficients by b_f and b_b , respectively. The irradiance ratio is denoted by R , and the shape factors for the incident and reflected photon streams by r_{dd} and r_{ud} , respectively. Finally, $\varepsilon_2 = (c - r_{dd}b_f)/(a + b_b)$. Gordon (1989) showed from Monte Carlo radiative transfer simulation that $\varepsilon_2 = 1.035$. For the clear sky condition in which the satellite remote sensing is feasible, photons just below the sea surface can be dominated by those from the direct Sun beam incident on the sea surface. In such a case $\mu_d \approx \cos(\theta_{sw})$ where θ_{sw} and μ_u represent the zenith angle of the apparent solar zenith angle just below the sea surface and the

average cosine for the upward riddance field, respectively. When $\cos(\theta_{sw})$ just below the sea surface is calculated from θ_s by $\sqrt{1 - \frac{\sin^2 \theta_s}{n^2}}$ using the Snell's law, substitution of Eq. 9 in to 7 and the resultant equation into Eq. 5 gives:

$$\overline{K_{PAR}(z)} = 1.339 \cdot \frac{1 - 0.201 \cdot \exp(-0.043 \cdot \theta_s)}{\sqrt{(1 - \sin^2 \theta_s) / n^2}} [a(490) + b_b(490)] \quad (10)$$

where the index of refraction n of seawater relative to air may be assumed 1.33. Eq. 10 indicates that $\overline{K_{PAR}}$ is essentially proportional to $a(490) + b_b(490)$, with the proportionality factor being a function of the solar zenith angle.

Substituting Eq. 10 into 2 finally gives $z_{1\%}$:

$$z_{1\%} = \frac{k_0 \sqrt{(1 - \sin^2 \theta_s) / n^2}}{[1 - k_1 \exp(k_2 \cdot \theta_s)]} \cdot \frac{1}{[a(490) + b_b(490)]} \quad (11)$$

where $k_0=3.003$, $k_1=0.201$, $k_2=-0.043$ in this study. Thus, $z_{1\%}$ is obtained once $a(490)$, $b_b(490)$ and θ_s is known. The former two ($a(490)$ and $b_b(490)$) are derived from the Inherent Optical Property algorithm (see ATBD for GCOM-C/SGLI IOP algorithm, otherwise Smyth et al., 2006), while the last can be obtained once time (year, month, date) and observation location is known (the code is embedded within the GCOM-C/SGLI IOP algorithm).

3. Algorithm evaluation

Fig.4 shows an example of $z_{1\%}$ derived from Eq. 9, using the NOMAD data set (Werdell and Bailey, 2005) from which simultaneous measurements of in situ $z_{1\%}$ and IOPs can be obtained. Also plotted are $z_{1\%}$ derived from other models of $K_d(\lambda)$ using $z_{1\%} \sim 4.605 / K_d(490)$. Statistics are summarized in Table 1. Eq. 9 performs relatively well with RMSE=23.7m, although some scatters are found compared to other models. The regression slope of Eq. 9 (and of Lee et al, 2005) is relatively close to 1.0, too.

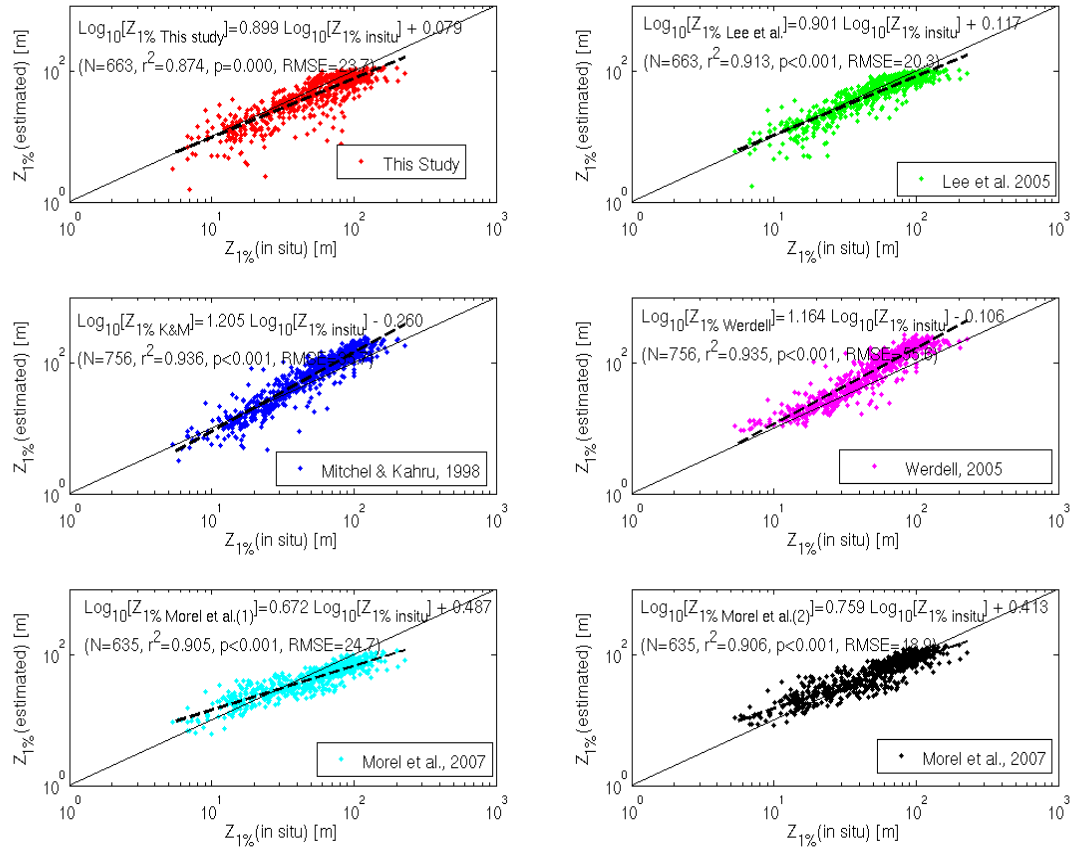


Fig. 4 Comparison between $z_{1\%}$ observed(x) and modeled (y), as well as between Eq.9 (this study) and other models.

Table 1. Statistical results of algorithm evaluation for a_{dy} against in situ data

	Slope#	Intercept#	RMSE*
Eq.9 (This study)	0.899	0.079	23.7
Lee et al., 2005	0.901	0.117	20.3
Mitchel & Kahru, 1998	1.205	-0.260	35.7
Werdell, 2005	1.164	-0.106	55.6
Morel et al., 2007A	0.672	0.487	24.7
Morel et al., 2007B	0.759	0.413	18.0

#log scale, *Liner scale

5. Algorithm calibration

When the statistical coefficients (the slope and intercept in Table 1) obtained for Eq. 9 is used to calibrate the algorithm, $z_1\%calib=(z_1\%-0.079)/0.899$. When the SGLI is actually launched and the algorithm uses the SGLI satellite signal, the calibration coefficients should be re-determined.

References

Hirata T. and N. Højerslev, Relationship between the irradiance reflectance and inherent optical properties of seawater, 113, C03030, doi:10.1029/2007JC004325,2008

Mitchell, B.G., M. Kahru, Algorithms for SeaWiFS standard products developed with the CalCOFI bio-optical data set. Calif. Coop. Oceanic Fish. Invest. Rep. 39, 133-147, 1998

Lee, Z.-P., K.-P. Du, and R. Arnone, A model for the diffuse attenuation coefficient of downwelling irradiance, J. Geophys. Res., 110, C02016, doi:10.1029/2004JC002275, 2005.

Morel, A., Antoine, D., and B. Gentili, Bidirectional reflectance of oceanic waters: Accounting for Raman emission and varying particle phase function, Appl. Opt., 41, 6289-6306, 2002.

Morel, A., Y., Huot, B., Gentili, P. J., Werdell, S. B. Hooker, B. A. Franz, Examining the consistency of products derived from various ocean colour sensors in open ocean (Case 1) waters in the perspective of a multi-sensor approach, Remote Sens. Environ., 111, 69-88, 2007.

Smyth, T.J., G. F. Moore, T. Hirata, J. Aiken, Semianalytic model for the derivation of ocean color inherent optical properties: description, implementation, and performance assessment, Appl. Opt., 45, 8116-8131, 2006.

Werdell, J., http://oceancolor.gsfc.nasa.gov/REPROCESSING/SeaWiFS/R5.1/k490_update.html, 2005

Werdell, P. J. and S. W. Bailey, An improved in situ data set for bio-optical algorithm development and ocean color satellite validation, Remote Sens. Environ., 98, 122-140, 2005